Dynamics of the Ganglion Cell Response in the Catfish and Frog Retinas

MASANORI SAKURANAGA, YU-ICHIRO ANDO, and KEN-ICHI NAKA

From the National Institute for Basic Biology, Okazaki 444, Japan, and Canon Research Center, Atsugi 243-01, Japan

ABSTRACT Responses were evoked from ganglion cells in catfish and frog retinas by a Gaussian modulation of the mean luminance. An algorithm was devised to decompose intracellularly recorded responses into the slow and spike components and to extract the time of occurrence of a spike discharge. The dynamics of both signals were analyzed in terms of a series of first- through third-order kernels obtained by cross-correlating the slow (analog) or spike (discrete or point process) signals against the white-noise input. We found that, in the catfish, (*a*) the slow signals were composed mostly of postsynaptic potentials, (*b*) their linear components reflected the dynamics found in bipolar cells or in the linear response component of type-N (sustained) amacrine cells, and (*c*) their nonlinear components were similar to those found in either type-N or type-C (transient) amacrine cells. A comparison of the dynamics of slow and spike signals showed that the characteristic linear and nonlinear dynamics of slow signals were encoded into a spike train, which could be recovered through the cross-correlation between the white-noise input and the spike (point process) signals. In addition, well-defined spike correlates could predict the observed slow potentials. In the spike discharges from frog ganglion cells, the linear (or first-order) kernels were all inhibitory, whereas the second-order kernels had characteristics of on-off transient excitation. The transient and sustained amacrine cells similar to those found in catfish retina were the sources of the nonlinear excitation. We conclude that bipolar cells and possibly the linear part of the type-N cell response are the source of linear, either excitatory or inhibitory, components of the ganglion cell responses, whereas amacrine cells are the source of the cells' static nonlinearity.

INTRODUCTION

In the vertebrate retina, ganglion cells, a class of typical Golgi type-I cells, make a long-distance communication by means of action potentials carried along their long axons. This is in contrast to the other retinal interneurons, which process and transmit signals by means of graded potentials, either depolarization or hyperpolarization. Although ganglion cells have been studied extensively in the

Address reprint requests to Dr. Ken-Ichi Naka, National Institute for Basic Biology, Okazaki, 444 Japan.

J. GEN. PHYSIOL. © The Rockefeller University Press · 0022-1295/87/08/0229/31 $2.00

Volume 90 August 1987 229–259

past, the cells' response dynamics have been studied by only a few workers (Knight et al., 1970; Victor et al., 1977; Victor and Shapley, 1979). The dynamics of intracellularly recorded responses have not been analyzed. Such an analysis is difficult because (*a*) the cells' response is composed of two components, spike and slow potentials, and (*b*) the amount of information carried by a spike train is limited. Recently, we (Sakuranaga and Naka, 1985*a–c*) analyzed signal transmission within catfish retina by means of a white-noise stimulus and a cross-correlation technique and showed that the signal transmissions or transfer functions among preganglionic cells could be identified by the characteristic linear and nonlinear kernels. In this article, we will segregate the ganglion cell response into spike (discrete or point process) and slow (analog) potentials, and extend the white-noise analysis to spike trains to determine the dynamics of the ganglion cell response. The dynamics of a few selected cells will be fully analyzed to establish an analytical routine. We do not intend to make an extensive survey of ganglion cells based on their response dynamics. This subject will be dealt with in the near future. As the spike train is the ubiquitous means of information transmission in the central nervous system, the applicability of the methodology we have developed here is not limited to the visual systems.

The major conclusions we have drawn for catfish ganglion cells are as follows. (*a*) The dynamics of a spike train can be defined in a short experimental run of <60 s. (*b*) The lower-order kernels describe the dynamics of the intracellularly recorded slow potentials as well as of spike trains. (*c*) The linear component was from either bipolar or type-N (sustained) amacrine cells and the nonlinear components were from type-C (transient) and type-N (sustained) amacrine cells. (*d*) The dynamics of slow potentials were transferred to the spike trains without major alterations. (*e*) Well-defined spike correlates of slow potential corresponding to an action potential were obtained. If similar correlates are produced at the synapses made by the ganglion cell axons, the postsynaptic cell will be able to reconstruct the information contained in the slow potentials of the ganglion cell.

Analyses performed on extracellularly recorded spike trains from frog ganglion cells showed that, in the frog, (*a*) the linear components were inhibitory, whereas the (second-order) nonlinear components produced on-off transient excitation, and (*b*) the analysis of the nonlinear components suggested two amacrine cell types, sustained and transient.

We suggest that ganglion cells receive two parallel inputs, one linear and the other nonlinear, from bipolar and amacrine cells, a conclusion drawn for cat retinas by Hochstein and Shapley (1976), and that ganglion cell spikes were generated as a signal follower for preserving the signals produced within the retina.

MATERIALS AND METHODS

Experiments were done with eyecup preparations of the channel catfish, *Ictalurus punctatus*, and the bullfrog, *Rana catesbeiana*, obtained locally. Recordings were made intracellularly from catfish ganglion cells by glass microelectrodes filled with 2 M potassium citrate and extracellularly from frog ganglion cells by platinum-coated tungsten electrodes. The light stimulus was a Gaussian white-noise modulation around a mean luminance, and

covered the entire retina. The light source was a Sylvania glow tube (R-1113C, Sylvania/GTE, Exter, NH) and the Gaussian white-noise signal was obtained from a signal generator (WG-772, NF Circuit Block, Tokyo, Japan). The light stimulus was monitored by a photodiode before it was attenuated by a series of neutral density filters. For each spike discharge from a frog retina, a Schmidt trigger circuit produced a unitary pulse of 4 ms in duration. The input (light signal) and output (cellular responses) were initially stored on analog tape and digitized onto the computer at a digitization rate of 4 or 8 kHz. Ganglion cells were identified by their large spike activities for the intracellular recordings. Catfish cells that produced spike discharges of small amplitudes were not used. In all, 14 on-center and 28 off-center catfish ganglion cells and 67 frog ganglion cells were analyzed.

Here we will briefly describe the analysis performed on the slow (analog) potential and the extension of such an analysis to spike trains (point process) that we have developed. The visual stimulus, $L(t)$, in general has two components, a mean luminance, I_0, that can be assumed constant, and a modulation, $i(t)$, whose time average must be zero:

$$L(t) = I_0 + i(t). \tag{1}$$

The resulting responses recorded intracellularly from ganglion cells were composed of two components, analog (slow potential) and discrete (spike train) signals. The analog signal had two components, a steady membrane polarization, V_0, and a time-varying part, $v(t)$:

$$V(t) = V_0 + v(t). \tag{2}$$

In the second-order approximation, the dynamic part, $v(t)$, is expressed by convolving the first- and second-order kernels, $h_1(\tau)$ and $h_2(\tau_1, \tau_2)$, with the stimulus to give (Sakuranaga et al., 1986):

$$v(t) = \int_0^\infty h_1(\tau)i(t - \tau)d\tau + \int_0^\infty \int_0^\infty h_2(\tau_1, \tau_2)i(t - \tau_1)i(t - \tau_2)d\tau_1 d\tau_2. \tag{3}$$

The linear dynamics, given by the first integral in the right-hand side of Eq. 3, are a temporal superposition of the responses produced by input modulation, $i(t)$; the nonlinear dynamics, given by the second term, show a deviation from a linear superposition of the responses produced by inputs, arriving at a time coulisse of $\tau_1 - \tau_2$.

The first- and second-order kernels are computed by cross-correlating the slow component of response against the stimulus modulation as:

$$h_1(\tau) = (1/P)\overline{v(t)i(t - \tau)}; \tag{4a}$$

$$h_2(\tau_1, \tau_2) = (1/2P^2)\,\overline{[v(t) - V_0]i(t - \tau_1)i(t - \tau_2)}. \tag{4b}$$

Here the bar denotes an average over time t, and P represents the spectral density of the stimulus modulation. Note that the steady potential, V_0, and the kernels, $h_1(\tau)$ and $h_2(\tau_1, \tau_2)$, vary with mean luminance, a parametric change described as field adaptation by Rushton (1965). Such changes probably have their origin in the outer retina (Chappell et al., 1985; Naka et al., 1987). The detailed algorithms for computation and intuitive interpretations of kernels are shown elsewhere (Sakuranaga and Naka, 1985*a*, *b*).

Intracellular recordings from a ganglion cell were separated into an analog (slow potential) process and a point (spike) process by means of an algorithm that was implemented in the software program STAR. This algorithm separates two signals automatically from single intracellular recordings, provided that the recordings preserved large-amplitude spike potentials.

The dynamics of a spike train, recorded extracellularly or extracted from intracellular recording, were analyzed similarly. Fig. 1 schematically illustrates a cross-correlation

technique used for analog and discrete (spike train) signals. In the latter case, the kernels are not related to the time of occurrence of spike discharges, but to the spike density function, the probability of spike generation (see Appendix). The first- and second-order kernels have respective units of millivolts times seconds times centimeters^2 per microwatt and millivolts times seconds^2 times centimeters^4 per microwatt^2 for the analog signal, and spikes times centimeters^2 per microwatt and spikes times seconds times centimeters^4 per microwatt^2 for the spike (point process) signal.

All analytical routines are implemented in a software system, STAR, running on a combination of a VAX 11/780 (Digital Equipment Corp., Maynard, MA) and AP120B array processor (Floating Point Systems, Portland, OR).

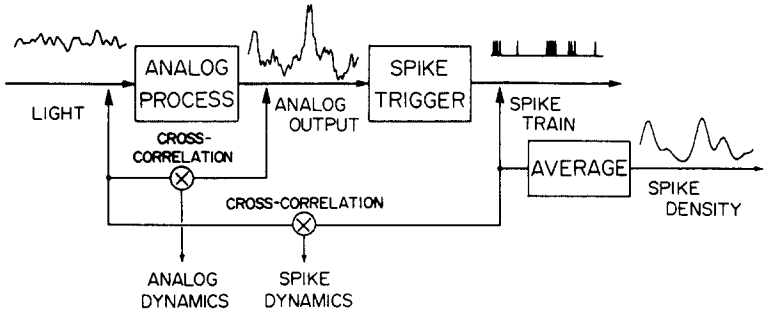

FIGURE 1. A schematic representation of the cross-correlation technique. A white-noise–modulated input produces analog signals, which trigger a spike train at the output stage, the ganglion cells. Cross-correlation is made between the input and the analog signal or between the input and the spike signal. The former defines the dynamics of the analog output, and the latter describes the dynamics of the averaged spike trains evoked by a repetition of the same input.

RESULTS

White-Noise Modulation and Ganglion Cell Response

Photic stimuli in the natural environment always have a mean luminance, and complete darkness, often used as the background in intracellular recordings from retinal neurons, is a special case of the zero mean level. Responses evoked by a step and by white-noise–modulated light inputs are compared to provide a rationale for our use of white noise as a stimulus and of the complex analytical technique. Fig. 2 shows the responses from ganglion cells of catfish (*A*) and frog (*B*) evoked by a step of light, given in the dark, followed by white-noise–modulated light whose mean luminance corresponded roughly to the magnitude of the step input. The response in the catfish retina was recorded intracellularly and that in the frog retina was recorded extracellularly. In catfish, the step of light produced a sustained hyperpolarization with a depolarizing rebound on which high-frequency spike discharges were superposed. The response seen during the early part of the white-noise stimulation was also a sustained hyperpolarization with very little response to modulation. These responses were produced by the sudden appearance of a mean illumination in the dark, but not, in the case of the white-noise stimulus, by its modulation. The frog cell produced typical on-off discharges to a step input and a burst of discharges to the onset of

the white-noise stimulus. Except for the initial burst, the cell remained silent for several seconds. The record in Fig. 2*C* was obtained 10 s after the beginning of the white-noise stimulation, which is shown in Fig. 2*A*. White-noise modulation produced, in contrast to the record from the early part of stimulation, very energetic transient depolarizations on which spike discharges were superposed. Similarly, the frog cell produced bursts of discharges to modulation (Fig. 2*D*). It took nearly 10 s for both catfish and frog cells to reach their dynamic steady states and to begin to respond to modulation.

A sudden exposure of a retina to a light, steady or modulated, begins the process of field adaptation, in which the neurons try to adjust their dynamic

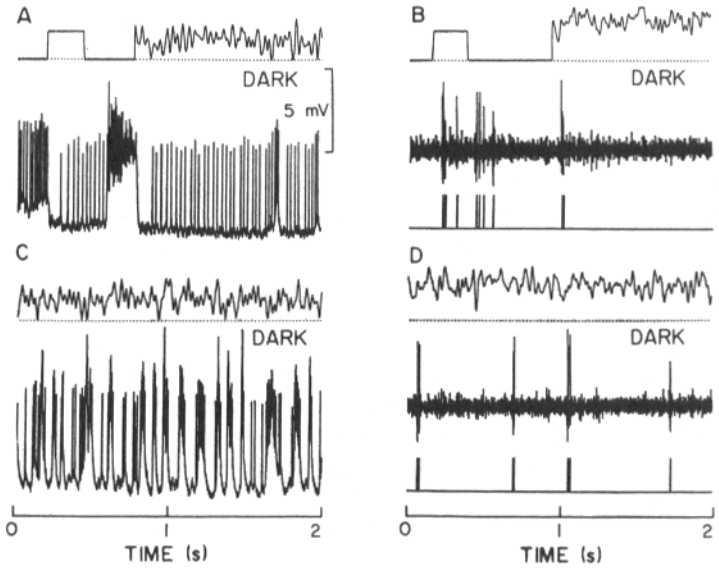

FIGURE 2. Responses evoked from a catfish and frog ganglion cell by a step and white-noise–modulated light. (*A* and *C*) Recorded intracellularly from a catfish off-center ganglion cell. *C* shows a record obtained 10 s after the beginning, in *A*, of the white-noise stimulation. (*B* and *D*) Recorded extracellularly from a frog on-off ganglion cell. *D* shows a record obtained 10 s after the end of *B*. In *B* and *D*, the third line shows unitized spike discharges. In *C* and *D*, the responses reached the dynamics steady state. Note the frequent transient depolarizations and discharges in *C* and brisk discharges in *D*.

sensitivity to the new mean luminance. Unless the stimulus is kept on long enough, a steady state is not achieved; otherwise, darkness returns before the retina is fully adapted to the new mean. Responses seen at the large and sudden onset of stimulus are nonstationary and reflect the transitory state of the retina. Such a transitory state has been seen in the turtle receptor, as well as in horizontal cells (Chappell et al., 1985; Naka et al., 1987), skate horizontal cells (unpublished data), cockroach ocellar neurons (Mizunami et al., 1986), and catfish retinal neurons (Sakuranaga and Naka, 1985*b*), and this state is a general property of the visual system. Continued stimulation by sinusoidal or white-noise modulation

around a mean brings retinal neurons into a stationary state: the retina is fully field (light) adapted and neurons in the outer retinas of turtle, catfish, and skate respond linearly to modulation around a mean luminance. We are concerned here with the dynamics of the ganglion cell response under such a dynamic steady state condition.

Visual inspection of the white-noise–evoked response, however, fails to give any intuitive understanding of the possible relationship between the input and output. As we reported previously (Sakuranaga and Naka, 1985*a–c*) and will reiterate later in this article, a precise input-output relationship can be found by performing a cross-correlation between the white-noise input and the resulting neuronal responses. Analyses were done through cross-correlation between the white-noise stimulus and cellular responses in the steady state as shown in Fig. 2, *C* and *D*.

Two Types of Intracellular Signals

Fig. 3 shows an intracellularly recorded response from a catfish off-center ganglion cell evoked by a white-noise–modulated light. The stimulus, marked "light" and denoted $L(t)$, had two components: a steady mean, I_0, and a temporal modulation, $i(t)$, as formulated in Eq. 1. The intracellular response consists of two components: a train of action potentials (a discrete signal on top of fluctuating slow potentials), and an analog signal (slow potentials). Spike discharges encode information as their time of occurrence, whereas slow potentials encode information as their instantaneous amplitude. Intracellular responses, therefore, are a mixture of two kinds of signals that have to be segregated for their response dynamics and interrelationships to be analyzed fully.

The original intracellular response in Fig. 3 was first differentiated to produce the difference trace in the same figure. The process of differentiation removed the slow potential components, and both the initiation and cessation of an action potential were easily detected as sharp deflections from the baseline. The trace marked "slow" in the figure was obtained by a linear interpolation between the initiation and cessation of a spike deflection and subsequently smoothed by a filter. In *B*, the details of our interpolation are illustrated by the dotted line, which was made by expanding the latter part of the response trace in *A*, and the slow component was smoothed in the bottom trace of *B* by filtering with a corner frequency of 50 Hz. The spike trace in Fig. 3*A* shows the time of occurrence, corresponding to a set of midpoints between the initiation and cessation of spike discharges (the response trace in the figure). Thus, an intracellular response (Fig. 3*A*) was segregated into two components, the slow potential component (slow trace) and the discrete component (spike trace).

Previously, intracellular ganglion cell responses that contained both slow and spike potentials or ganglion cell discharges were used to perform an input-output analysis (Naka et al., 1975). This procedure, however, does not allow us to compute the higher-order kernels because the two signals are intercontaminated. The algorithm presented here automatically separates the two signal components. The slow potential can be analyzed by means of the standard white-noise analysis without any contamination from the spike discharges, and simultaneously the

discharge pattern can be compared with the dynamics of the slow component. This allows us to identify transfer functions of spike-generating cells.

The power spectra shown in Fig. 4 were computed from a recording, a part of which is shown in Fig. 3, to confirm the segregation of two response components. The spectrum of the light stimulus was almost flat from near DC to ~50 Hz or more, whereas the spectrum of the recorded response extended over 1 kHz. The output response included harmonics at frequencies greater than that

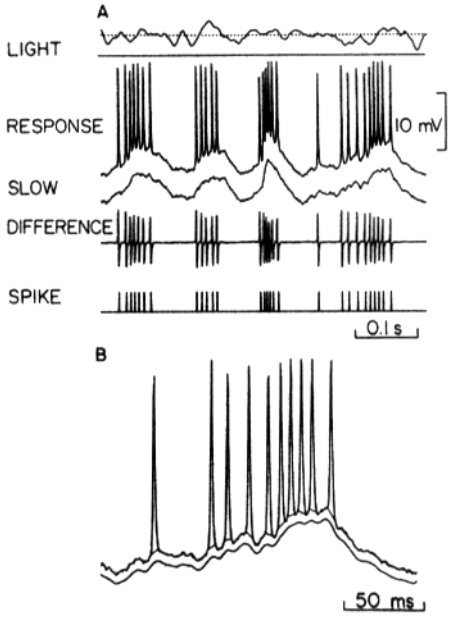

FIGURE 3. Time record of responses from a catfish off-center ganglion cell evoked by a white-noise–modulated field of light. (*A*) The light stimulus is a modulation around a mean luminance of 5 $\mu W/cm^2$, by $L(t)$ in Eq. 1. The response recorded intracellularly consists of an undulating slow potential ("slow") and a train ("spike") of action potentials. The record marked "response" is differentiated to produce the trace marked "difference." The slow and spike traces, denoted by $V(t)$ in Eq. 3 and $w(t)$ in Eq. 6, respectively, are segregated from the response trace based on its differentiation (difference trace) and on an algorithm developed in the text. (*B*) A part of the record, the response trace in *A*, is expanded (solid line), and a linear interpolation (dotted line) is made between the initiation and cessation of spikes. The smoothed slow potential, obtained by filtering, is shown below.

contained in the input modulation frequency. There are several factors that produce such higher frequencies: (*a*) the high-frequency components from individual spike potentials with their fast rising and falling phases, (*b*) noisy membrane potential fluctuations, and (*c*) spontaneous spike discharges uncorrelated to inputs.

The slow potential component obtained by the linear interpolation and smoothing shown in Fig. 3 has a power spectrum with a gentle peak at ~10 Hz, and the

spectrum decayed abruptly beyond 10 Hz. The slow potential shows a bandpass characteristic that is a feature common to all ganglion cells in catfish (see also Fig. 17). Up to ~50 Hz, the power of the slow potential component was nearly identical to that of the recorded response. The power spectrum of the spike component had a peak at 10 Hz, in addition to a second peak at 100–200 Hz. The frequency of the second peak differed from cell to cell because the spectrum was contaminated by the high-frequency components in each spike discharge, whose patterns and amplitudes differed from cell to cell.

One common measure of the discharge pattern is the interspike interval (or spike frequency) histogram of a spike train. The white-noise–modulated input provided a standard criterion for the comparison of discharge frequency patterns because the modulation has a uniform frequency characteristic. We found some

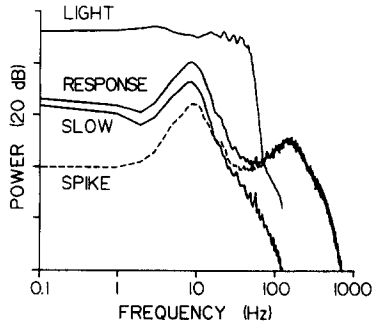

FIGURE 4. Power spectra of the response of a catfish off-center ganglion cell evoked by white-noise–modulated light. The time records of the responses are shown in Fig. 3. The input spectrum ("light") has almost uniform frequency components from near DC to ~80 Hz, while the response spectrum extends to frequencies over 1 kHz. The spectrum of the slow component is computed from the slow component of responses segregated as in Fig. 3, and it decays monotonically with a roll-off frequency of ~10 Hz. The waveform of the spike discharges is extracted by subtracting the slow trace from the response trace of Fig. 3, and its power spectrum is shown by the spike trace. Note that the spectrum has two gentle peaks at ~10 and ~200 Hz.

variants of discharge patterns in the responses of catfish ganglion cells to white-noise–modulated light. Fig. 5 shows two typical examples. The histogram in *A*, from the record shown in Fig. 3, has a single sharp peak at ~10 ms (100 Hz) with a tail over 100 ms (10 Hz). The histogram in *B*, from another catfish ganglion cell, shows a more complex discharge pattern: two sharp peaks at ~7 and ~20 ms (147 and 500 Hz) and a diffuse hump at ~70 ms (17 Hz). The first two peaks are due to two modes of multiple spike firing; the third is due to spontaneous discharges or to rhythmic spike bursts. The results in Figs. 4 and 5 describe some aspects of the response characteristics of the slow and spike components but fail to define the dynamic relationship between input and output. Two problems were associated with analysis of spike discharges: (*a*) the static response, which is represented by the average firing rate, was superimposed on

the dynamic response, which is correlated to the input modulation (see Appendix), and (*b*) the dynamic response could not be distinguished from the static response because of the stochastic character of spike discharges. A more precise analysis is needed to segregate the statics and dynamics or the linear and nonlinear components in the response.

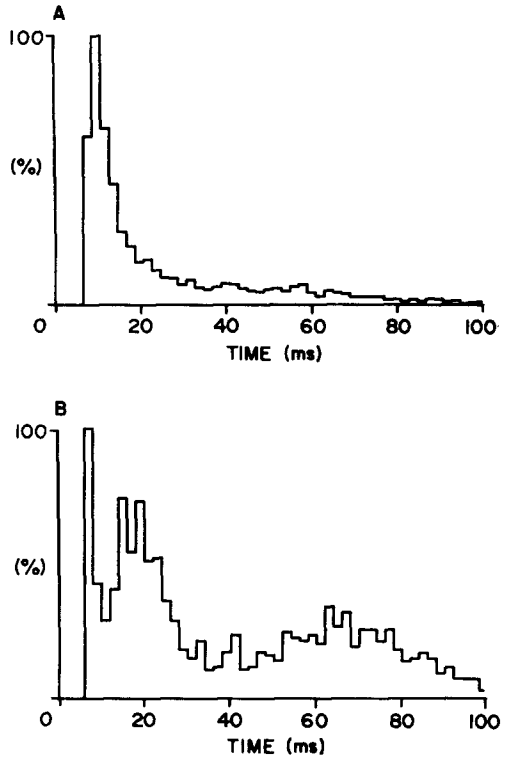

FIGURE 5. Interspike interval histograms of spike discharges of two catfish ganglion cells evoked by white-noise–modulated light. (*A*) Histogram from the spike discharges shown in Fig. 3. The histogram has a peak at ~10 ms (100 Hz) produced by a multiple-spike burst, with a tail over 100 ms (10 Hz). (*B*) A histogram from another ganglion cell shows a more complex character; it has three peaks at ~8, 20, and 70 ms with decreasing sharpness. The first and second peaks indicate paired and multiple spiking, and the third indicates a clustering of spike bursts.

Slow Component of Response

Fig. 6 shows a response from a catfish off-center ganglion cell evoked by a white-noise–modulated light. The slow component was extracted from the observed response by removing the spike component by the process described above. We computed the first- and second-order kernels by cross-correlating the slow response ("slow") against the input ("light"). From the kernels, we further extracted the linear component of the response by convolving the first-order kernel against the stimulus, as shown in Eq. 3. The linear prediction, marked

"first-order," apparently deviated from the observed slow component of the response. The magnitude of the deviation was 72%, which was estimated from the mean square error (MSE) between the observed and predicted slow response. The deviation is due to (*a*) the nonlinearity involved and (*b*) passive fluctuation of membrane potentials not correlated to the input. The second-order trace shows a part of the response predicted by the first- and second-order kernels. With the inclusion of the second-order nonlinearity, the MSE was reduced to 34% and the predicted response was similar to the slow potential component of the actual response. The cell's response had a considerable degree of second-order nonlinearity: the MSE was 38%. As was the case with type-N and type-C cells, the segregated slow component from ganglion cells probably includes a

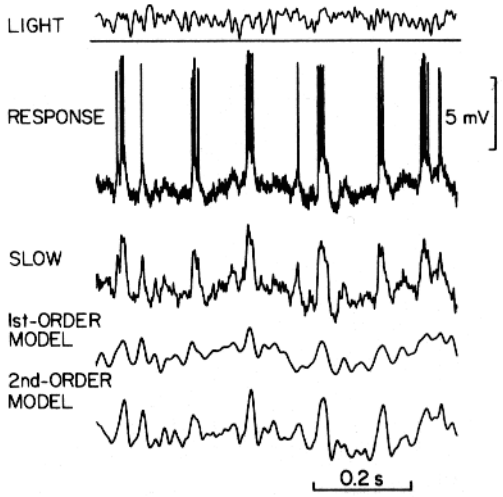

FIGURE 6. Time record of response of a catfish off-center ganglion cell evoked by a white-noise–modulated field of light. The stimulus has a mean luminance of 5 $\mu W/cm^2$. The slow component is extracted from the observed response. The slow component is predicted by convolving the first- and second-order kernels, shown in Fig. 7, with the light stimulus. The first-order prediction has an MSE of 72%; the inclusion of second-order component improves the MSE to 34%.

higher-order nonlinearity than the second-order and intrinsic noise uncorrelated to inputs, and produced a power spectrum similar to those from preganglionic cells (see Fig. 17).

Fig. 7, *A* and *B*, shows the first- and second-order kernels for a catfish off-center ganglion cell. In *A*, the first-order kernel was biphasic: a hyperpolarization followed by a depolarization. This is a characteristic common to the off-center ganglion cells. The on-center ganglion cells produced kernels with the opposite polarity (see Fig. 10*A*). Note that the first-order kernel in *A* resembles the kernels of off-center bipolar cells (Figs. 9 and 12 in Sakuranaga and Naka, 1985*a*) or of type-NB amacrine cells (Fig. 7 in Sakuranaga and Naka, 1985*b*). The cell had a well-defined second-order kernel, shown in Fig. 7*B*, which had a "three-eye"

configuration: a depolarizing peak on the diagonal and two off-diagonal hyperpolarizing valleys. A cut of the kernel made along the diagonal is also shown in Fig. 7*A*. The diagonal cut, in which $\tau_1 = \tau_2$, shows the nonlinearity owing to two pulses given concurrently, and the diagonal peaks, therefore, are the nonlinearity due to a single pulse. The off-diagonal component, on the other hand, is due to the interaction of modulated inputs at two different times. In Fig. 7*C*, step-

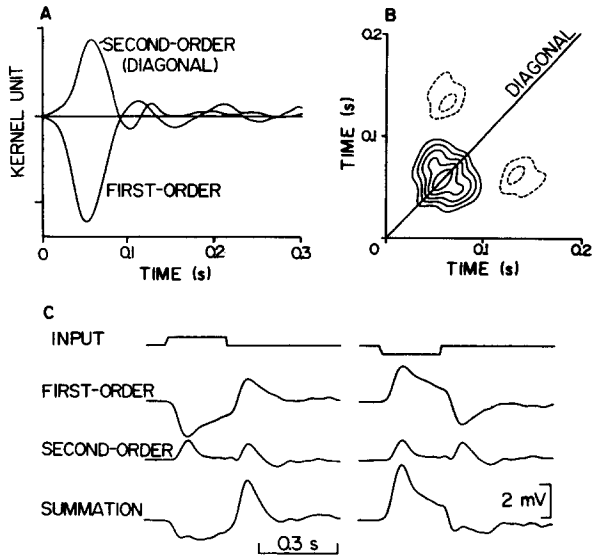

FIGURE 7. Kernels of the slow response component of a catfish off-center ganglion cell and their step-evoked responses. Parts of the response time records are shown in Fig. 6. The first-order kernel and the diagonal cut of the second-order kernel are shown in *A*. In *B*, the second-order kernel is displayed with contour lines: the solid lines show depolarizing nonlinearity and the dashed lines show hyperpolarizing nonlinearity. The kernel has the three-eye configuration: a peak on the diagonal and two valleys in the off-diagonal region. Step responses predicted from the kernels in *A* and *B* are shown in *C*. The first-order predictions from the first-order kernel show bandpass-filtered responses, which are mirror images of each other for stimuli of opposite polarity. The second-order predictions from the second-order kernel are identical for the two stimuli because the second-order nonlinearity is quadratic. The summation of the two predictions reproduces an asymmetry in the responses by the incremental and decremental steps. The contour lines in the second-order kernel show the magnitude of the nonlinear interaction.

evoked responses are predicted from these kernels. The first-order kernel predicted a bandpass response with opposite polarities for the incremental and decremental step inputs. The second-order kernel produced identical on-off transient responses for both the incremental and decremental steps because of the quadratic nonlinearity. This type of nonlinearity was found in the response of type-C amacrine cells (Sakuranaga and Naka, 1985*c*), in which the induced second-order kernels had three- or four-eye configurations. The summation of

the responses induced by both first- and second-order kernels showed a typical off-center response to an incremental or decremental step of light. The off response, therefore, included two types of responses: a (linear) bandpass response and a (nonlinear) on-off transient depolarization.

Linear and Nonlinear Signals in Slow and Spike Components

The standard approach to examining the dynamics of a spike train is to produce an analog signal or spike density function by averaging spike discharges produced by many repetitions of identical stimuli. Fig. 8*A* shows the responses from a catfish ganglion cell to incremental or decremental steps of light repeatedly delivered at a mean luminance ("light" trace). The intracellular response was decomposed into spike and slow potential components. Three sample traces of the times of occurrence of spike discharges are shown by the three traces marked "spike." The traces show similar but not exactly identical discharge patterns. The

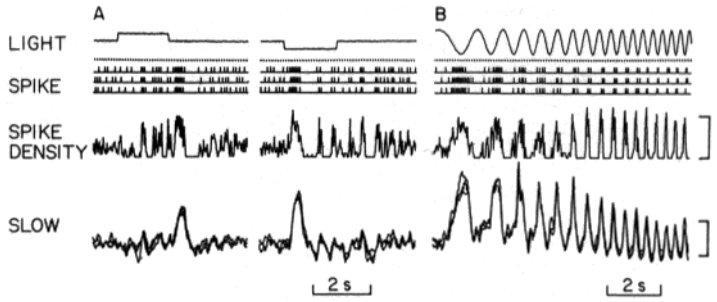

FIGURE 8. Responses of a catfish ganglion cell to incremental and decremental steps and sinusoidal modulation of light. The mean luminance was 5 $\mu W/cm^2$. The responses in *A* are produced by repeated steps of brightening and dimming and the responses in *B* are produced by repeated sinusoidal sweeps. The responses are separated into slow and spike components, and three representatives of each component are shown in a row (marked "spike") for the spike and by superimposition ("slow") for the slow component. Spike density functions of PST histograms were obtained by averaging spike discharges over 12 trials. The scales are 200 spikes/s for the spike density functions and 2 mV for the intracellular slow potentials.

difference among the discharge patterns was due partly to the jitter in the timing of the spike firing and partly to the fluctuations in the spontaneous activity. Spike trains were averaged over 12 trials for the incremental and decremental steps to produce post-stimulus time (PST) histograms (Fig. 8*A*, "spike density"). The original spike trains were a discrete signal, while their averaged response became an analog measure of the dynamics, the spike density function. The PST histograms were not very smooth but contained high-frequency components such as the sharp corners owing to the limited numbers of time bins and repetitions. Four sample traces for the slow potential components are superposed in Fig. 8 (trace marked "slow"). The slow potentials produced by four repetitions of an identical stimulus were not exactly identical, owing to intrinsic as well as extrinsic

noise. A comparison of the averaged spike train and slow potential component shows that a depolarization matches the increase of spike density, and a hyperpolarization corresponds to the decrease or suppression of spike activity. The incremental and decremental responses, either of slow or spike components, were not a mirror image of each other, which suggests that some nonlinearities were involved in the generation of both slow and spike components.

The experiment shown in Fig. 8*A* was followed by another series of repetitive stimulations by a light stimulus whose mean luminance was modulated by a sinusoidal sweep (Fig. 8*B*). Sinusoidal modulations produced cycles of both depolarizing slow potentials and spike bursts synchronous with the sinusoidal sweep. The synchronization between the light modulation and both responses suggested that the slow and spike components had a large linear component (see also Fig. 14). In quasilinear systems, sinusoidal inputs should produce roughly sinusoidal responses. There are three main features seen in the responses evoked by the sinusoidal inputs. (*a*) The responses, both slow potentials and spike discharges, were synchronous with the input modulation; one cycle of sinusoidal input produced one cycle of responses, which shows that both responses had a large linear components. (*b*) The sample spike records showed that no two discharge patterns were identical, although they were all evoked by identical stimuli. As shown in Fig. 8, there was a jitter in the firing of the discharges. (*c*) The slow potential became progressively smaller as the sinusoidal frequency increased, whereas the amplitude of the spike histogram became larger. The timing of spike firing was phase-locked statistically for the modulation of lower frequency, which shows that the relationship between the amplitude of depolarization and the firing of a discharge was statistical; i.e., the spike generator had a noise. The relationship became deterministic for the input of higher frequency, as seen from the sharp histograms with a large amplitude. Firing was tightly coupled with the input modulation.

Fig. 9*A* shows the results of an experiment in which a 45-s white-noise stimulus evoked an intracellular response from a catfish off-center ganglion cell and the response was decomposed into the analog (slow potential) and discrete (spike) components by the procedure we have already described. Cross-correlation of the white-noise input and the analog component defines the dynamics of the slow component: this is the standard white-noise analysis. We also cross-correlated the white-noise input against the discrete (spike) component to compute a spike kernel. Fig. 9*A* shows two first-order kernels, one computed from a slow component and the other from a spike component, which are similar in their waveforms although the discrete (spike) kernel had slightly shorter peak response times for both the initial hyperpolarizing phase and the following depolarizing rebound. This shows that the slow and spike components in the intracellular recording had similar linear dynamics. This observation was confirmed in Fig. 9*B* by Fourier transforms of both kernels to obtain gain and phase functions of the linear components. Both the slow and spike transfer functions showed bandpass characteristics having a gentle peak at ~10 Hz in the gain plot and an increasing delay of phase with the increase in the modulation frequency. The transfer functions for the slow and spike components differed slightly. The spike

component showed relatively greater amplification and its phase was more advanced than that of the slow component for frequencies above 1 Hz. These results show (*a*) that the correlation between the white-noise input and discrete (spike) signal produces a first-order kernel similar to the one produced by the standard analog-to-analog white-noise analysis, and (*b*) that there were no substantial differences in the linear dynamics of the slow and spike responses.

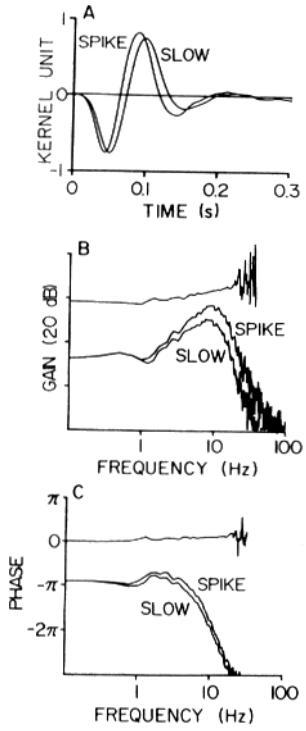

FIGURE 9. First-order kernels and transfer functions of slow and spike responses recorded from a catfish off-center ganglion cell. (*A*) First-order kernels of both types of signals are generated by cross-correlating output signals with a white-noise–modulated light. Both signals produce biphasic and almost identical kernels, indicating bandpass character. (*B*) Transfer functions, gain and phase, are computed for both slow and spike response components by Fourier transform of the kernels in *A*. The analog-to-digital transformation shows no substantial filtering, although a small increase was seen in both gain and phase at higher frequencies.

Fig. 10 compares the first-order kernels observed from many ganglion cells in catfish and frog. All the kernels were produced from white-noise stimulation of 45–60 s in duration. In *A* and *B*, the kernels were obtained from four on-center and four off-center catfish ganglion cells for their slow (solid line) and spike (dashed line) components. Both classes of cells showed biphasic first-order kernels: for the on-center cells, the kernels were initially depolarizing for the slow

signal and excitatory (an increase in the spike firing) for the spike signal; for the off-center cells, the kernels were initially hyperpolarizing and inhibitory (a decrease in the spike firing). In all cells, the kernels for the spike signal had a peak time slightly faster than the slow signal. This is because the spike kernel was more differentiating than the slow potential kernel, as noted in Fig. 9. Except for this difference, however, there was no substantial difference in the linear

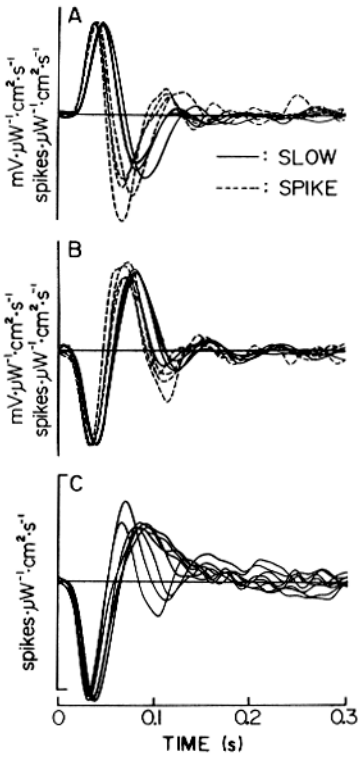

FIGURE 10. Comparison of first-order kernels from catfish and frog ganglion cells. Kernels were obtained from slow (solid line) and spike (dashed line) components of catfish ganglion cell responses; four on- and four off-center cells are shown in *A* and *B*, respectively. Note that the peak response time of the spike-induced kernels is faster and more differentiated than that of the slow potential-induced kernels. In *C*, kernels of spike discharges from eight frog ganglion cells are shown. All of the frog cells we examined produced kernels with an initial hyperpolarization (inhibition) followed by an afterdepolarization (excitation).

response dynamics of the slow potential and spike components. A simple straightforward relationship must exist between the membrane depolarization or hyperpolarization and the increase (excitation) or decrease (inhibition) in the spike discharge.

Discharges from frog ganglion cells were evoked by a white-noise–modulated stimulus of 45–60 s and cross-correlation was made between the white-noise

input and spike discharges transformed into the discrete signal. In the frog, discharges produced by a step of light given in the dark are classified into three patterns: on, off, and on-off discharges (Hartline, 1940). Step modulations of a mean luminance, and brightening or dimming from a mean luminance, produced mostly on-off discharges. We analyzed the spike responses from 67 frog ganglion cells, and all of the cells produced well-defined first-order kernels that were biphasic with the initial inhibitory (a decrease in discharge frequency) phase, as shown in Fig. 10*C*. We did not find any cells that produced a kernel with an initial excitatory phase. Although only a few intracellular recordings (not shown) from frog ganglion cells were examined, the slow potential and spike dynamics in frog ganglion cells were similar to each other, as shown for catfish in Fig. 10, *A* and *B*. Frog ganglion cells must therefore receive linear inputs from preganglionic cells, and the preganglionic cells must show an initial hyperpolarization for a step increment superposed on a steady mean luminance.

We discovered that two catfish amacrine cells, type-C and type-N cells, produced characteristic second-order kernels (Sakuranaga and Naka, 1985*b*, *c*). Fig. 11 shows second-order kernels from two catfish ganglion cells. In both cells, intracellularly recorded responses were segregated into two components, analog (slow potential) and discrete (spike) components. A second-order correlation between the white-noise stimulus and the resulting analog components is the standard procedure for producing a second-order kernel. The correlation produced two second-order kernels for the analog components shown in Fig. 11, *A* and *C*. The cross-correlation between the white-noise input and the discrete (spike) outputs produced the second-order kernels shown in Fig. 11, *B* and *D*. As in the case of the first-order kernels shown in Figs. 9 and 10, cross-correlation between the white-noise input and discrete signal produced second-order kernels very similar to those obtained by the standard procedure, which shows that a 60-s white-noise stimulation combined with the cross-correlation technique enabled us to recover the second-order nonlinearity from a spike train. The second-order kernels shown in Fig. 11, *A* and *B*, are characterized by a structure in which two peaks on the diagonal, where $\tau_1 = \tau_2$, and two valleys in the off-diagonal region, where $\tau_1 \neq \tau_2$, are located at the corners of a square. This is the four-eyed structure found in type-C (transient) amacrine cells of catfish retina (see Fig. 18*A*). The second-order kernels shown in Fig. 11, *C* and *D*, had an on-diagonal peak followed by alternating negative and positive ranges orthogonal to the diagonal. This is very similar to the structure found in type-N (sustained) amacrine cells in catfish retina (see Fig. 18*B*). Note that these characteristics of kernels were kept unchanged in the dynamics of spike trains from catfish ganglion cells.

The second-order correlation between the white-noise light stimulus and discrete (spike) signals from frog ganglion cells showed that the majority (~80%) of the frog ganglion cells had a second-order nonlinearity similar to the one found in catfish type-C amacrine cells; the remaining cells (~20%) produced kernels similar to the one found in catfish type-N cells. Fig. 12 shows two examples of second-order kernels produced from spike discharges of frog ganglion cells. The kernel in *A* had a structure similar to the one from catfish type-C amacrine cells, while the kernel in *B* had a structure similar to the one from

type-N cells. The figure also shows the responses to step inputs predicted by the two frog kernels. The incremental and decremental inputs both produced identical responses: this was because the second-order kernels were quadratic for inputs. The response predicted by the type-C kernel was a transient depolariza-

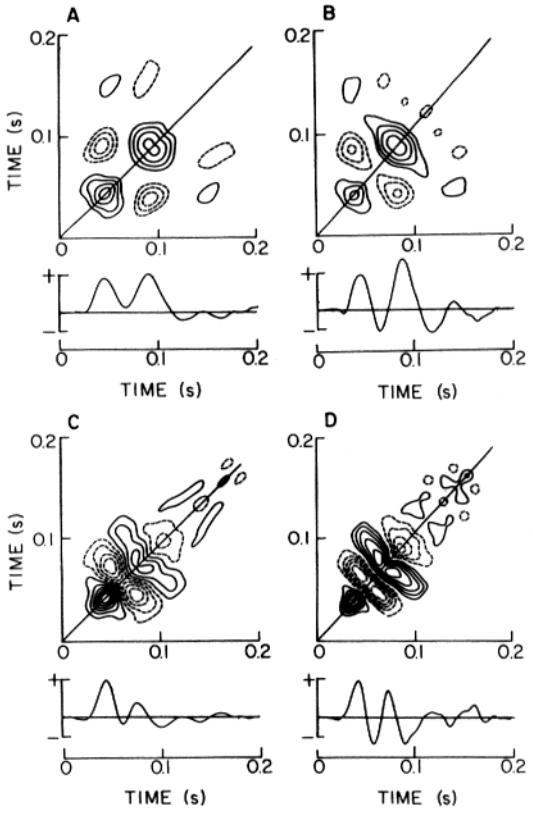

FIGURE 11. Second-order kernels of both slow and spike responses of catfish ganglion cells. *A* and *C* are slow potential–induced and spike-induced kernels from the same cell and are referred to as type-C kernels. Both kernels show four-eye configurations such that two peaks on the diagonal and two valleys in the off-diagonal region make four corners of a square. *C* and *D* are from another cell that produced N-type second-order kernels. The kernels are composed of alternating peaks and valleys orthogonal to the diagonal. Kernel profiles along the diagonal are shown under the horizontal time axis. In *A* and *C*, the solid contour is depolarizing and the dashed one is hyperpolarizing. Similarly, in *B* and *D*, the solid contour is excitatory (an increase in spike discharge) and the dashed one is inhibitory (a decrease in spike discharge). The contour lines show the magnitude of nonlinear interaction.

tion at the onset and offset of step inputs and should produce on-off discharges. The waveforms of the predicted response were very similar to the step-evoked responses from type-C amacrine cells in catfish or transient amacrine cells in other lower vertebrate retinas. The responses predicted by the type-N kernel were also on-off transients with a large undershoot (i.e., spike suppression). The

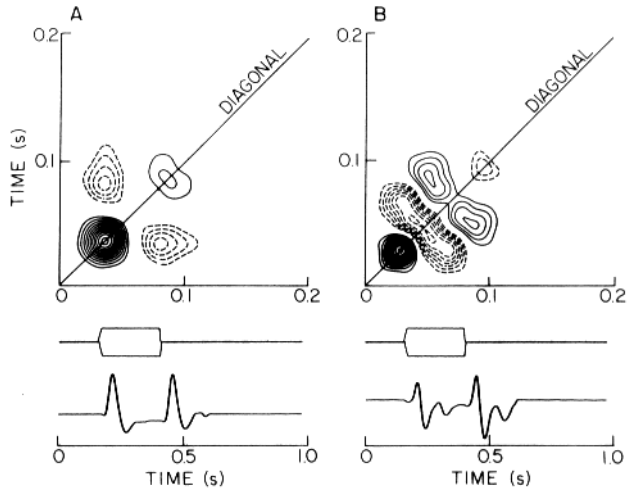

FIGURE 12. Two characteristic second-order kernels computed from frog ganglion cell spike discharges. *A* shows a C-type kernel and *B* shows an N-type kernel. Predictions by the kernels to incremental and decremental step inputs are also shown. As the second-order kernels are quadratic, two inputs produced identical responses. The contour lines show the magnitude of the nonlinear interaction.

differentiating on-off transients suggest that the ganglion cell with the type-N kernels generated more brisk on-off discharges and that the cell could respond better to two separate input pulses coming within a short interval.

Fig. 13 shows a typical example of the on-off discharges evoked from a frog ganglion cell by a brief flash of light superimposed on a steady mean luminance.

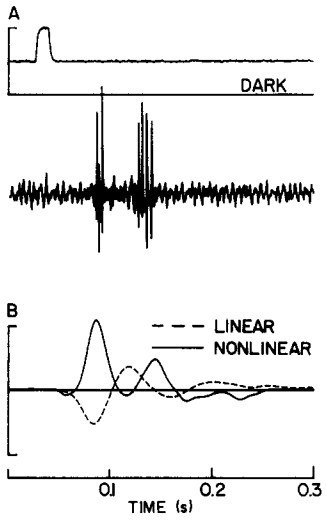

FIGURE 13. Frog ganglion cell discharges produced by a brief incremental flash (*A*) and the predicted linear and nonlinear components from the first- and second-order kernels (*B*). Predictions were obtained by convolving the kernels with the stimulus shown in *A*.

Also shown are the linear and nonlinear responses to the same flash of light predicted by the first- and second-order kernels from the same ganglion cell. For the onset of the stimulus, the linear component was induced by an inhibitory (hyperpolarizing) post-synaptic potential (PSP), whereas the excitatory (depolarizing) PSP generated the nonlinear component. The on discharges were therefore produced by the balance of these two opposing PSPs produced by the first- and second-order kernels. The off discharges were elicited by a synergistic action of the two components, since the discharges were produced during the excitatory phase of the linear and nonlinear components. On-off discharges produced by step inputs (superposed on a mean luminance) from frog ganglion cells were probably dominated by the second-order nonlinearity, and an interplay between (inhibitory) linear and (excitatory) nonlinear components may produce the complex discharges in the frog ganglion cells.

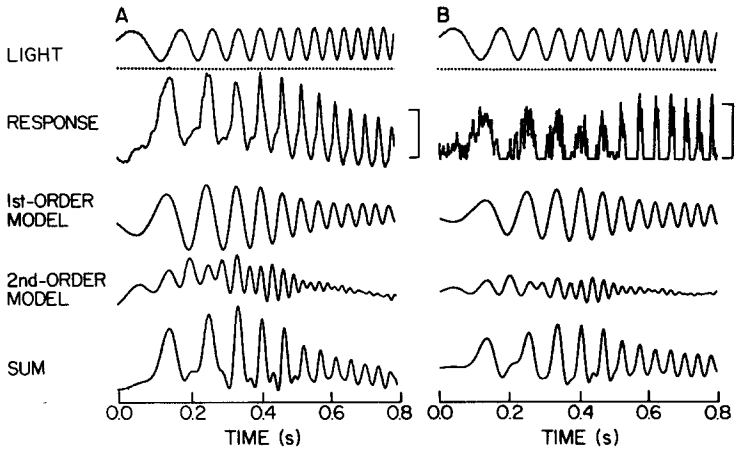

FIGURE 14. Slow and spike responses from a catfish ganglion cell to a sinusoidal modulated input. The slow response in *A* was obtained by averaging the actual responses shown in Fig. 8, and the spike density response in *B* was shown in Fig. 8. The model traces were predicted by convolving the first- and the second-order kernels with the stimulus marked "light." The summation trace ("sum") was produced by summing the first- and second-order model traces. The scales are 200 spikes/s for the spike density and 2 mV for the intracellular slow potential.

Fig. 14 shows the predictions made by the first- and second-order kernels for the slow (analog) and spike (discrete) responses evoked by a modulation of the mean luminance by sinusoidal sweep. Intracellular responses from a catfish ganglion cell were decomposed into the slow and spike components by the method shown in Fig. 3. The spike histogram is the same one shown in Fig. 8. The cellular responses, both slow and spike components, produced one cycle of response to each cycle of input modulation, which shows that these responses had a large linear component. The linear responses were predicted by convolving the sinusoidal sweep with the first-order kernels. For the slow potential component, the prediction is the best linear approximation of the intracellularly recorded response, and for the spike component, the prediction is the best linear approximation of the spike density function with a statistical phase-locking

character. Both linear predictions had a peak at ~10 Hz and show the bandpass characteristics (differentiating waveform) of the first-order kernels (Figs. 9 and 10). The power spectra shown in Fig. 17 clearly illustrate this bandpass characteristic.

The second-order responses were also predicted by convolutions of the input sinusoidal sweep with the second-order kernels, both of which were similar to those from type-C amacrine cells. The predicted second-order responses had a frequency doubling characteristic, and the summation of these linear and nonlinear responses mimicked the observed responses. The second-order response of the slow component had a depolarizing trend at ~3–10 Hz, but this was not reproduced by the second-order kernel of the spike component because of the weak differentiation during the slow-to-spike conversion. For the slow potential, the predicted response matched rather well with the recorded response, whereas for the spike potential, the match was not so good, particularly in the high-frequency region. In fact, an early study showed that the MSEs for the ganglion cell responses were between 20 and 50% (Naka et al., 1975). There are several reasons for the discrepancy between the prediction and the actual response: (*a*) more repetitions of stimuli are needed to average the jitter in the spike generation, and (*b*) higher-order nonlinear components were introduced in the slow-to-spike conversion. The sharp peaks and corners in the PST histogram at higher frequencies could not be reproduced by the second-order kernels, which indicates that the phase-locking contained high-order nonlinearities at faster modulation frequencies. As the input frequency increased, the phase-locking became less stochastic. This suggests that a sudden change in luminance, such as a step of light, must generate higher-order nonlinearity. The predictions by the first- and second-order kernels of step-evoked responses such as the ones shown in Fig. 8 were not good.

Correlate between Slow and Spike Signals

The similarity between the dynamic responses of the slow and spike components suggests a rather simple mechanism underlying the generation of spike discharges, which is an analog-to-digital conversion. The analog signal is the end product of signal processing in the retina and the discrete signal is transmitted to the brain. There may be a loss of part of the information originally contained in the slow potential during such a conversion. To examine these points, we sought a correspondence between the waveforms of slow potentials and spike trains by cross-correlating two signals. Fig. 15 shows the results in which cross-correlation was performed for the slow components and spike trains of ganglion cells, both evoked by white-noise–modulated light. This procedure is the same as taking an average of slow potentials triggered by spike discharges (randomly triggered average). The averaged slow potential is a correlate corresponding to an action potential in a statistical sense.

In all cases, the triggered spike timing shown by the vertical dotted line in Fig. 15 was followed by a depolarizing peak of the spike-correlated components of the slow potential. This was expected from the fact that the first-order kernels from the spike (discrete) components always had a shorter peak time than the

kernels from the slow potential components. This was probably due to factors such as the threshold for triggering a spike discharge and the bandpass (differentiation) filter between the slow and spike potentials. The waveforms of the spike correlates, however, differed from cell to cell: in some cells, hyperpolarization occurred before the spike trigger; in others, the depolarizing peak was followed by a hyperpolarization. In addition to the threshold and refractory period, there might be several dynamic factors related to the generation of spikes, because the depolarizing (upward) phase generates discharges more efficiently than the hyperpolarizing (downward) phase as seen in the rebound excitation. This is consistent with the observation that the spike-induced (first-order) kernel is more differentiated than the slow potential–induced kernel. Also, the spike generation may be coupled to some portion of slow potentials such as afterpotentials, either depolarization or hyperpolarization, and postspike depolarization (Marchiafava and Torre, 1977).

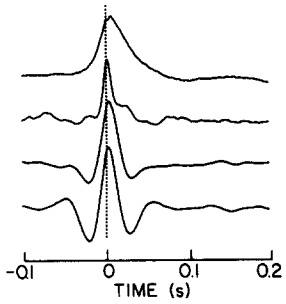

FIGURE 15. Slow potential correlates of spike discharges. Correlates were obtained by cross-correlating the slow component against the spike train evoked by a white-noise–modulated light. Each correlate is an average of slow potentials triggered by random spike discharges. The time origin shows the timing of single spikes. The top and bottom correlates are from two on-center cells and the middle two are from two off-center cells. Peak depolarizations were normalized.

The next question is whether the observed slow potentials could be reproduced from the time of occurrence of the spike discharges and the spike correlates. Fig. 16 shows the results of such a reproduction. An intracellular response, a part of which is shown in Fig. 16, was evoked by a white-noise stimulus ("light" trace). The response was segregated into the slow (analog) and spike (discrete) components. A correlation was made between the spike and slow potential components and spike correlates were obtained. One spike correlate was produced for each time of occurrence of a spike discharge, as shown in Fig. 16 ("correlate"). Spike correlates were linearly summed to produce the trace marked "model" in Fig. 16, which is the slow potential predicted by the correlates and times of occurrence of the spike discharges. The two traces, the observed and predicted slow potentials, are similar but not identical. Indeed, the MSE for the two slow potentials was 32.7%. The difference may be due to several factors: (*a*) the spike correlates were obtained statistically, and (*b*) there could have been (subthreshold) potential changes that did not produce any spike potential. To test the second possibility,

we computed the differences between the slow trace and the model trace and counted the number of the spikes that were missed in the observed responses in spite of the spike correlates. We found that the correlates produced 95% of the spike discharges, whereas the remaining 5% were spike discharges produced without any correlates. This indicates that the spike discharges were generated not only by overcoming the threshold but also by detecting spike correlates in the slow undulation observed in the ganglion cell's response. This observation fits an integrate-and-fire model where the slow-to-spike transduction is accomplished by an integrate-and-fire generator. We tried a similar reconstruction of slow potentials from the spike correlate but found that the reconstruction was not always satisfactory. The most important factor for successful reconstruction was to keep the normal discharge during intracellular recordings. In the catfish,

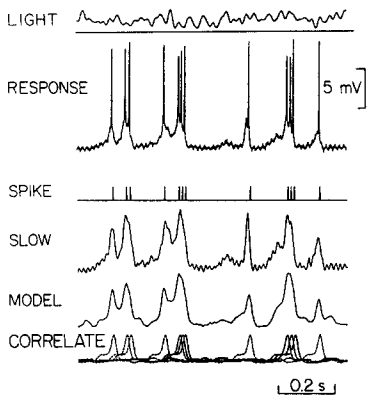

FIGURE 16. Response from a ganglion cell evoked by a white-noise–modulated light and its reconstruction by superposition of spike correlates. The stimulus ("light"), with a mean of 5 $\mu W/cm^2$, evoked a response that was separated into a spike train and a slow undulation. The spike correlate was computed by a cross-correlation between the slow and spike traces, and a series of correlates was placed where spikes were seen ("correlate"). The sum of the correlates ("model") is a prediction by the correlates of the real response shown in the slow trace. The voltage calibration is for the response trace, and the other slow potentials were expanded twice vertically.

penetration of a ganglion cell by an electrode often induced an excess depolarization that induced an abnormally high spike firing frequency or depressed spike firing completely.

DISCUSSION

Ganglion cells are the final output of the vertebrate retina. Morphologically, most ganglion cells receive two kinds of synaptic inputs: one from the bipolar cells, whose responses are produced by signals processed in the outer retina, and the other from amacrine cells, whose responses are produced by signals processed in the inner retina (Dowling and Boycott, 1966; Werblin and Dowling, 1969). Cells in the outer retina, including bipolar cells, produce a dynamic response that is linearly related to a modulation around a mean luminance, whereas a

similar stimulus produces characteristic nonlinear responses from amacrine cells (Naka et al., 1975; Sakuranaga and Naka, 1985*a–c*). The difference in the response characteristics of the bipolar and amacrine cells in catfish provides a means to analyze the inputs to the ganglion cells.

Spike discharges carried along the axons of the ganglion cells are the end product of the complex signal processing in the vertebrate retina. These discharges are triggered by the excess depolarization produced by an interplay of excitatory and inhibitory PSPs generated by bipolar and amacrine cells (Marchiafava, 1976; Naka, 1977; Marchiafava and Torre, 1977; Thibos and Werblin, 1978; Baylor and Fettiplace, 1979; Belgum et al., 1982). Generation of an action potential is, of course, a highly nonlinear process, and the potential contains high-frequency components that are not related to information carried by the potential. An action potential itself does not carry any information, but the timing of spike occurrence does.

Responses from retinal neurons are produced by two components in the light stimulus, the steady mean luminance and the dynamic modulation around the mean. Hyperpolarization of a receptor or horizontal cell at one particular moment, for example, could be elicited either by a mean luminance or by a sinusoidal or white-noise modulation. By separating the evoked responses into static and dynamic components (Chappell et al., 1985; Naka et al., 1987), the part of a stimulus that produces a response was determined. Similarly, the input-output relationship of ganglion cells has to be defined in terms of the statics and dynamics of the cell's response. For a spike train, the statics are determined by the average firing frequency and the dynamics are determined by the temporal pattern of discharges (see Appendix).

Two problems are involved in analyzing the dynamics of the spike trains: (*a*) the trains are a point process with a maximum firing frequency of <1 kHz to limit the amount of information carried by the trains; (*b*) the firing of a spike discharge is a stochastic process and there is always a jitter in the time of occurrence of a discharge. The former indicates that signals are transmitted only intermittently, and the latter indicates that no two spike trains produced by two identical stimuli are identical. The standard means for analyzing the dynamics of spike train is to produce PST histograms of discharges produced by repeating many identical stimuli (Gerstein and Kiang, 1960; Kiang et al., 1965). A PST histogram is therefore a spike density function. Although the dynamics of a spike train can be appreciated intuitively from PST histograms, the responses cannot be decomposed into linear and nonlinear components and their dynamics are difficult to analyze. The time when a discharge occurs has to be sorted into bins with a finite temporal width. This process introduces artificially high-frequency components not contained in the original spike trains. To minimize this effect, the bin's width has to be made smaller or a histogram has to be low-pass-filtered to produce a smooth function. The former choice requires a longer experimental time, whereas the latter involves an appropriate choice of a filter.

It is, however, possible to produce a PST histogram by repeating the (pseudo-random) white-noise stimulus, which is cross-correlated against the input to produce a series of kernels (Marmarelis and Naka, 1973). Although this method enables us to identify the dynamics of spike trains, three difficulties are involved;

two have been mentioned and the third is the long span of recording time because the same white-noise stimulus has to be repeated to produce a histogram. However, as shown mathematically in the Appendix, repetition of white-noise stimulation is not essential to generate the first- and second-order kernels for the spike density function. A single sweep of white-noise stimulus of <60 s produces well-defined first- and second-order kernels, as shown in Figs. 9–12. This method is an extension of the standard white-noise technique to systems with discrete outputs.

In the past, several attempts were made to analyze the dynamics of spike trains. The most straightforward approach is the trigger or reverse correlation in which the average (optimal) input waveform to trigger a spike discharge is sought (Boer and Kuyper, 1968; Eggermont et al., 1983). Schellart and Spekreijse (1972) determined the dynamics of ganglion cell discharges with this approach. The correlation function in the trigger correlation is identical to the first-order kernel in this article but is interpreted differently.

Bryant and Segundo (1976) interpreted the kernels as the stimulus pattern, the transmembrane current in their case, to generate most efficiently a spike discharge. Their interpretation is applicable to the systems with an analog output such as a slow potential, but there is no a priori reason to apply the interpretation to the generation of a single spike discharge. The first-order kernels we obtained here are the linear component of the PST histogram (i.e., the spike density function), produced by an impulse input, such as a flash superposed on a mean luminance. The second-order kernels show a deviation from linearity in the spike density function. The kernels (Naka, 1977) obtained by cross-correlating the pulse-shaped spikes with white-noise–modulated current injected into several interneurons can be interpreted similarly.

Victor et al. (1977) and Victor and Shapley (1979) obtained first- and second-order kernels in the frequency domain by correlating an input, a sum of sinusoids, against spike discharges from cat ganglion cells. They postulated a sandwich model in which a static nonlinearity was sandwiched between two linear filters. The first linear filter was assumed to be the bipolar cells. Our observations in this article lead to a similar conclusion. The source of the static nonlinearity was assumed to be the amacrine cells. Here we have shown that the nonlinearities found in catfish and frog ganglion cells were similar to those found in type-C and type-N amacrine cells in catfish. Our recent analysis has shown that the type-C nonlinearity could be produced by a (linear) bandpass filter followed by a static nonlinearity, which is a squaring function. The nonlinearity found in type-N cells could also be produced if the output of type-C amacrine cells were followed by another linear filter. This scheme is identical to the one proposed for the cat by Victor and Shapley.

Spike generation has usually been discussed in relation to the threshold current, which produces an all-or-none firing of an action potential in a cell. The threshold of a cell changes only gradually and has been assumed to be essentially static. Little is known about the dynamic properties of spike generation, except for accommodation reported in turtle ganglion cells (Baylor and Fettiplace, 1979). We found that spike discharges in a ganglion cell have a well-defined correlate of slow potential, and can be modeled by an integrate-and-fire generator. Such

a correlate differs from cell to cell, but is probably produced by an interplay of PSPs. Reciprocal connections between ganglion cells and preganglionic (bipolar and amacrine) cells, reported recently by Sakai et al. (1986), may contribute to making a correlate a booster in triggering spikes dynamically. These findings also suggest an interesting hypothesis: if a spike conducted along the axon of a ganglion cell reaches a postganglionic cell and produces a PSP whose waveform

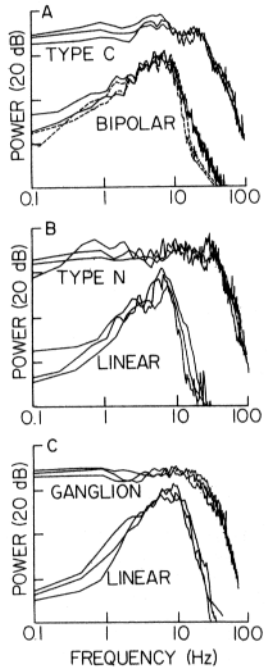

FIGURE 17. Power spectra of the responses evoked by a white-noise–modulated light. (*A*) Power spectra of responses from three type-C amacrine cells and from two bipolar cells, an on-center and an off-center cell. The dashed lines are the power spectra of the linear model response predicted by the first-order kernel. (*B*) Power spectra from two type-NA and two type-NB amacrine cells. Their responses were decomposed into linear and nonlinear components. The power spectra of linear components are marked "linear." (*C*) Power spectra of the slow response component from an on-center and two off-center ganglion cells. Their responses were also decomposed to linear and nonlinear components for computing their spectra. Note that the linear spectra of ganglion cells resembled those of bipolar and type-N amacrine cells and power spectra of ganglion cells resembled those of type-C and type-N amacrine cells.

is very similar to the spike correlate of the slow potential found in the ganglion cell, the postsynaptic cell can reconstruct the slow potential observed in the ganglion cell. In this case, spike discharges are a messenger of analog-to-analog signal transmission. This hypothesis further suggests the possibility that there is no loss of information at the analog-to-digital signal transmission in the ganglion cell.

In Fig. 17 comparisons are made in power spectra between responses evoked

from several types of catfish retinal neurons by white-noise–modulated light. The spectra, in *C*, of the linear part of the ganglion cell's slow response were very similar to those, in *A*, of the responses observed from bipolar cells and those, in *B*, of the linear responses from type-N amacrine cells. The higher-frequency component of the slow response of the ganglion cell was not seen in the response of the bipolar cells but was present in the response of type-N and type-C amacrine cells. The dynamics of preganglionic cells were transmitted and reproduced in the slow potentials in the ganglion cells. This supports the view that slow potentials are composed mostly of PSPs driven through forward or reciprocal pathways between bipolar or amacrine cells and ganglion cells (Dowling and Boycott, 1966).

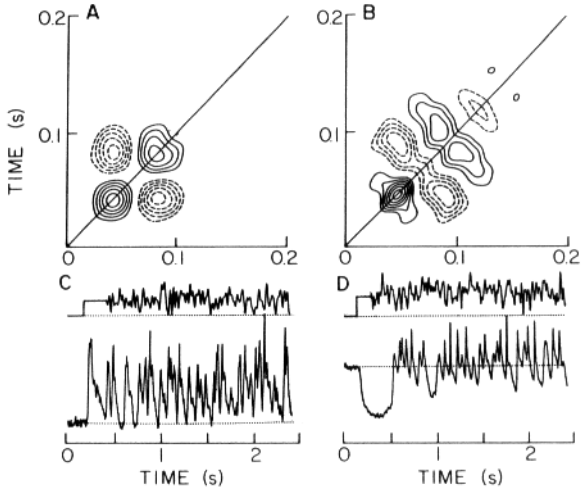

FIGURE 18. Two characteristic second-order kernels from catfish amacrine cells. The kernel in *A* was from a type-C (transient) amacrine cell and that in *B* was from a type-N (sustained) amacrine cell. The responses from these cells are also shown (*C* and *D*). The contour lines show the magnitude of the nonlinear interaction.

The most important conclusion in this article is that the first- and second-order response characteristics of catfish ganglion cells remain substantially unchanged during the analog-to-digital signal conversion. This is probably true for frog ganglion cells, although we do not have sufficient data to confirm it. We showed (Sakuranaga and Naka, 1985*a–c*) that the characteristics of signal transmission in catfish retinal interneurons were reproduced by a series of lower-order kernels. A characteristic nonlinearity appeared when the signals in the outer retina were transmitted to the two amacrine cells and the nonlinearity was identified by the second-order kernels. Fig. 18 shows two types of second-order kernels, from a type-C (transient) amacrine cell (*A*) and from a type-N (sustained) amacrine cell (*B*). The former was referred to as a C-type kernel and the latter as an N-type kernel. We found the same types of kernels in slow potentials (PSPs) of catfish ganglion cells and in spike discharges of catfish and frog ganglion cells. The present findings, therefore, show that spike trains of ganglion cells carry

information about the characteristics of signals transacted within the retina. We also found two minor but definite characteristics in the slow potential to spike conversion: (*a*) the weak differentiation seen in the first- and second-order kernels, and (*b*) the deterministic phase-locking produced by faster modulation.

In the catfish, current injection into bipolar or type-N amacrine cells produces discharges from ganglion cells (Naka, 1977). A white-noise–modulated current injected into bipolar cells produced depolarizing, monophasic first-order kernels from ganglion cells. Similarly, a current injected into type-N amacrine cells induced monophasic first-order kernels with a sign-inverting or sign-noninverting character from ganglion cells. Because of these low-pass transfer functions (equivalent to the monophasic kernels), the response dynamics of bipolar or type-N amacrine cells were transmitted to the ganglion cells without much transformation. The present study also shows that type-C amacrine cells must be communicating with ganglion cells because the second-order nonlinearity found in some ganglion cells was similar to that found in type-C amacrine cells. The nonlinearity is characterized by the three- or four-eye structure of the second-order kernels in Figs. 7*C* and 11. Although there may be exceptions, such nonlinearities may be mediated mostly through type-C amacrine cells. Several authors (Frumkes et al., 1981; Belgum et al., 1982) suggested an inhibitory effect from transient amacrine to ganglion cells. If the transmission is inhibitory or sign-inverting, the second-order kernel of ganglion cells must have a polarity opposite to that of the second-order kernels from type-C amacrine cells. Our findings, however, showed that the polarity of second-order kernels in catfish and frog is the same in both the type-C amacrine and ganglion cells. The transmission is sign-noninverting or excitatory.

We conclude that, in catfish ganglion cells, (*a*) linear components originate in bipolar cells and/or type-N amacrine cells and (*b*) nonlinear components originate in type-N or type-C amacrine cells. There are parallel inputs, linear and nonlinear, to the ganglion cells in the catfish retina, similar to the signal flow proposed by Hochstein and Shapley (1976) in the cat retina. The ganglion cell pools the signals transacted within the retinal interneurons, but makes no substantial signal transformations in producing slow potentials and therefore spike trains. Ganglion cells are a simple signal-follower, making an optimal PSP-to-spike or analog-to-digital conversion.

Frog ganglion cells, on the other hand, are known to respond to complex visual stimuli and to produce very complex responses such as movement detection (Lettvin et al., 1959). Much circumstantial evidence has suggested that transient amacrine cell activity underlies the generation of such complex responses in ganglion cells (Dowling, 1968; Werblin, 1977; Ariel and Daw, 1982). However, direct evidence for this conjecture is lacking. In the present study, we identified the linear and nonlinear components underlying the generation of ganglion cell discharges. The second-order nonlinearities from frog ganglion cells were very similar to those found in catfish amacrine cells of either type N or type C. Although such a nonlinearity may be produced in frog ganglion cells themselves, it seems most plausible that (*a*) there are two types of amacrine cells in frog retina and (*b*) these cells are the primary source of complex excitation to the on-

off ganglion cells. This proposition is in agreement with our conclusion for catfish ganglion cells. In addition, transient and sustained amacrine cells have also been found in goldfish (Kaneko, 1973), turtle (Marchiafava and Weiler, 1982), and mudpuppy (Frumkes et al., 1981; Coleman, 1983). A recent study (Watanabe and Murakami, 1984) on intracellular responses from frog ganglion cells has also shown that complex signal processing takes place in preganglionic cells.

Although the excitation of frog ganglion cells is dominated by a nonlinear depolarizing input, there is also a linear and inhibitory input to the cells. The linear input may have been produced by signals from the sustained amacrine cells, as indicated in the mudpuppy (Frumkes et al., 1981), but was probably produced by signals from (off-center) bipolar cells as well. In the frog retina, a small number of ganglion cells was found to receive dual synaptic inputs, one from bipolar cells and the other from amacrine cells, at the ribbon synapses (Dowling, 1968). The first-order kernels observed from frog ganglion cells were very similar to those found in catfish bipolar or type-N amacrine cells. On-off ganglion cells in the frog are also known to be inhibited by annular illumination (Barlow, 1953), and the linear inhibitory input we have observed in the responses of these cells may reflect this surround inhibition.

The present study has shown that the response dynamics in catfish and frog ganglion cells are similar. In a ganglion cell, the linear and nonlinear components that originate in bipolar and amacrine cells are combined. The ratio of the two components indigenous to each cell produces a variety of response patterns.

APPENDIX

An action potential is all-or-none and its information is carried to postganglionic cells by the timing of its occurrence. A train of spike discharges may thus be considered a point process. Such a process is expressed by a train of delta functions, $\delta(\cdot)$, as:

$$w(t) = \sum_j \delta(t - t_j). \tag{5}$$

Here t_j represents the time of spike occurrence. Practically, $w(t)$ is replaced by a sequence of unit pulses with a short duration. The times of occurrence of spike discharges evoked by identical stimuli are, in general, not identical but are statistically fluctuating. The standard means for analyzing the dynamics of a spike train with such jitters is to produce a PST histogram by averaging the number of spikes falling into time bins over many responses by repeating identical stimuli (Gerstein and Kiang, 1960; Kiang et al., 1965). In an earlier study, Marmarelis and Naka (1973) applied such a scheme for analyzing spike trains of a ganglion cell evoked by white-noise stimulation. This is formulated as follows. If we observe repeated spike trains many times, e.g., K times, stimulating by the same sweep of a white-noise modulation, the timing of the spike trains may differ from sweep to sweep. The point process is defined with relation to the trial, k, as:

$$w_k(t) = \sum_j^k \delta(t - t_{jk}). \tag{6}$$

Here t_{jk} represents the occurrence of kth trial. The spike density function is defined by averaging the point processes over the trials:

$$U(t) = (1/K)\sum_k w_k(t). \tag{7}$$

Here the summation is taken over all the trials. As in the case of the slow component

expressed in Eq. 2, the response of spike density consists of a steady mean, U_0, and a time-varying component, $u(t)$:

$$U(t) = U_0 + u(t). \tag{8a}$$

The static part, U_0, is equal to the average firing rate, which varies with mean luminance, I_0. The dynamic part is expressed in the second-order approximation as:

$$u(t) = \int_0^\infty g_1(\tau)i(t-\tau)d\tau + \int_0^\infty\int_0^\infty g_2(\tau_1, \tau_2)i(t-\tau_1)i(t-\tau_2)d\tau_1 d\tau_2. \tag{8b}$$

The kernels, $g_1(\tau)$ and $g_2(\tau_1, \tau_2)$, also vary with mean luminance and are obtained by cross-correlating the spike density against the stimulus as:

$$g_1(\tau) = (1/P)\overline{u(t)i(t-\tau)}; \tag{9a}$$

$$g_2(\tau_1, \tau_2) = (1/2P^2)\overline{[u(t) - U_0]i(t-\tau_1)i(t-\tau_2)}. \tag{9b}$$

This algorithm for kernel computation is the same as that used by Marmarelis and Naka (1973). The right-hand side of Eq. 9 is further simplified because the time averages, $\overline{w_k(t)i(t-\tau)}$ and $\overline{w_k(t)i(t-\tau_1)i(t-\tau_2)}$, can be averaged across trials because of the assumed stationarity of the response. Then the kernels in Eq. 9 are reduced to a simplified form:

$$g_1(\tau) = (1/P)\overline{w(t)i(t-\tau)}; \tag{10a}$$

$$g_2(\tau_1, \tau_2) = (1/2P^2)\overline{[w(t) - U_0]i(t-\tau_1)i(t-\tau_2)}. \tag{10b}$$

This shows that the first- and second-order kernels for spike density can be computed in the same way as for the analog signal in Eq. 4. There is no need to estimate explicitly the spike density function generated by repeating an identical white-noise sweep. The spike train evoked by a single sweep of white-noise stimulation (<60 s in duration) enables us to obtain the first- and second-order kernels. The first-order kernel thus obtained is similar to the impulse function produced by the trigger (or reverse) correlation (Boer and Kuyper, 1968; Schellart and Spekreijse, 1972; Eggermont et al., 1983). Our final expression of Eq. 10 becomes identical to that given by Bryant and Segundo (1976) when $w(t)$ in the right-hand side of Eq. 10 is replaced by that of Eq. 5. They assumed the kernels were proportional to a best-stimulus pattern, transmembrane current in their case, to elicit a spike discharge in a cell. Although their interpretation is correct for analog output, e.g., analog potential or spike density function, there are no a priori reasons to extend their assumption to impulse generation. The strictest interpretation of spike-induced kernels is that they are a comprehensive representation of spike density function: the first-order kernel is the best linear approximation and the second-order kernel is the best second-order (nonlinear) approximation of the spike-density function (PST histogram) produced by an impulse input. The first-order kernels also represent a kind of statistical phase-locking character because the kernel produces a sinusoidal spike density to sinusoidal inputs. At an extreme of the deterministic phase-locking dynamics, the spike density becomes a sharp peak to an input sinusoid: higher-order kernels contribute to the reproduction of such a spike density.

We thank Hiroko M. Sakai for her valuable comments on the manuscript. We also thank two referees of the *Journal* for improving greatly the original manuscript.

This research was partly supported by National Institutes of Health grant EY-01897.

Original version received 12 March 1986 and accepted version received 14 January 1987.

REFERENCES

Ariel, M., and N. W. Daw. 1982. Pharmacological analysis of directionally sensitive rabbit retinal ganglion cells. *Journal of Physiology.* 324:161–175.

Barlow, H. B. 1953. Summation and inhibition in the frog's retina. *Journal of Physiology.* 119:69–88.

Baylor, D. A., and R. Fettiplace. 1979. Synaptic drive and impulse generation in ganglion cells of turtle retina. *Journal of Physiology.* 288:107–127.

Belgum, J. H., D. R. Dvorak, and J. McReynolds. 1982. Sustained synaptic input to ganglion cells of mudpuppy retina. *Journal of Physiology.* 326:91–179.

Boer, E. de., and P. Kuyper. 1968. Trigger correlation. *IEEE Transactions on Biomedical Engineering.* BME-15:169–179.

Bryant, H. L., and J. P. Segundo. 1976. Spike initiation by transmembrane current: a white-noise analysis. *Journal of Physiology.* 260:279–314.

Chappell, R. L., K.-I. Naka, and M. Sakuranaga. 1985. Dynamics of turtle horizontal cell response. *Journal of General Physiology.* 86:423–453.

Coleman, P. 1983. Morphological and physiological study of the interactions between excitation and inhibition in mudpuppy inner retina. PhD. thesis. The City University of New York, New York. 172 pp.

Dowling, J. E. 1968. Synaptic organization of the frog retina: an electron microscopic analysis comparing the retinas of frogs and primates. *Proceedings of the Royal Society of London, Series B.* 170:205–227.

Dowling, J. E., and B. B. Boycott. 1966. Organization of the primate retina: electron microscopy. *Proceedings of the Royal Society of London, Series B.* 166:80–111.

Eggermont, J. J., P. I. M. Johannesma, and A. M. H. J. Aertsen. 1983. Reverse-correlation methods in auditory research. *Quarterly Reviews of Biophysics.* 16:341–414.

Frumkes, T. E., R. F. Miller, M. Slaughter, and R. F. Dacheux. 1981. Physiological and pharmacological basis of GABA and glycine action on neurons of mudpuppy retina. Amacrine-mediated inhibitory influences on ganglion cell receptive-field organization: a model. *Journal of Neurophysiology.* 45:783–804.

Gerstein, G. L., and N. Y. S. Kiang. 1960. An approach to the quantitative analysis of electrophysiological data from single neurons. *Biophysical Journal.* 1:15–28.

Hartline, H. K. 1940. The receptive field organization of optic nerve fibers. *American Journal of Physiology.* 130:700–711.

Hochstein, S., and R. M. Shapley. 1976. Linear and non-linear spatial subunits in Y cat retinal ganglion cells. *Journal of Physiology.* 262:265–284.

Kaneko, A. 1973. Receptive field organization of bipolar and amacrine cells in the goldfish retina. *Journal of Physiology.* 235:133–153.

Kiang, N. Y. S., T. Watanabe, E. C. Thomas, and L. F. Clark. 1965. Discharge Patterns of Single Fibers in the Cat Auditory Nerve. MIT Press, Cambridge, MA. 451 pp.

Knight, B. W., J.-I. Toyoda, and F. A. Dodge, Jr. 1970. A quantitative description of the dynamics of excitation and inhibition in the eye of *Limulus*. *Journal of General Physiology.* 56:421–437.

Lettvin, J. Y., H. R. Maturana, W. S. McCulloch, and W. H. Pitts. 1959. What the frog's eye tells the frog's brain. *Proceedings of the Institute of Radio Engineers.* 47:1940–1951.

Marchiafava, P. L. 1976. Centrifugal actions on amacrine and ganglion cells in the retina of the turtle. *Journal of Physiology.* 255:137–155.

Marchiafava, P. L., and V. Torre. 1977. Self-facilitation of ganglion cells in the retina of the turtle. *Journal of Physiology.* 268:335–351.

Marchiafava, P. L., and R. Weiler. 1982. The photoresponses of structurally identified amacrine cells in the turtle retina. *Proceedings of the Royal Society of London, Series B.* 214:403–415.

Marmarelis, P. Z., and K.-I. Naka. 1973. Nonlinear analysis and synthesis of receptive-field responses in the catfish retina. I. horizontal cell-ganglion cell chain. *Journal of Neurophysiology.* 36:605–618.

Mizunami, M., H. Tateda, and K.-I. Naka. 1986. Dynamics of cockroach ocellar neurons. *Journal of General Physiology.* 88:275–292.

Naka, K.-I., P. Z. Marmarelis, and R. Y. Chan. 1975. Morphological and functional identifications of catfish retinal neurons. III. Functional identification. *Journal of Neurophysiology.* 38:92–131.

Naka, K.-I. 1977. Functional organization of catfish retina. *Journal of Neurophysiology.* 40:26–43.

Naka, K.-I., M. Itoh, and R. L. Chappell. 1987. Dynamics of turtle cones. *Journal of General Physiology.* 89:321–337.

Rushton, W. A. H. 1965. The Ferrier lecture, 1962: visual adaptation. *Proceedings of the Royal Society of London, Series B.* 162:20–46.

Sakai, H. M., K.-I. Naka, and J. E. Dowling. 1986. Ganglion cell dendrites are presynaptic in the catfish retina. *Nature.* 310:495–497.

Sakuranaga, M., and K.-I. Naka. 1985*a*. Signal transmission in the catfish retina. I. Transmission in the outer retina. *Journal of Neurophysiology.* 53:373–389.

Sakuranaga, M., and K.-I. Naka. 1985*b*. Signal transmission in the catfish retina. II. Transmission to type-N cell. *Journal of Neurophysiology.* 53:390–410.

Sakuranaga, M., and K.-I. Naka. 1985*c*. Signal transmission in the catfish retina. III. Transmission to type-C cell. *Journal of Neurophysiology.* 53:411–428.

Sakuranaga, M., S. Sato, E. Hida, and K.-I. Naka. 1986. Nonlinear analysis: mathematical theory and biological applications. *CRC Critical Reviews in Biomedical Engineering.* 14:127–184.

Schellart, N. A. M., and H. Spekreijse. 1972. Dynamic characteristics of retinal ganglion cell response in goldfish. *Journal of General Physiology.* 59:1–21.

Thibos, L. N., and F. S. Werblin. 1978. The response properties of the steady antagonistic surround in the mudpuppy retina. *Journal of Physiology.* 278:79–99.

Victor, J. D., and R. M. Shapley. 1979. Receptive field mechanisms of cat X and Y retinal ganglion cells. *Journal of General Physiology.* 74:275–298.

Victor, J. D., R. M. Shapley, and B. W. Knight. 1977. Nonlinear analysis of cat retinal ganglion cells in the frequency domain. *Proceedings of the National Academy of Sciences.* 74:3068–3072.

Watanabe, S., and M. Murakami. 1984. Synaptic mechanisms of directional selectivity in ganglion cells of frog retina as revealed by intracellular recordings. *Japanese Journal of Physiology.* 34:485–495.

Werblin, F. S. 1977. Regenerative amacrine cell activity and formation of on-off ganglion cell response. *Journal of Physiology.* 264:767–786.

Werblin, F. S., and J. E. Dowling. 1969. Organization of retina of the mudpuppy, *Necturus maculosus.* II. Intracellular recording. *Journal of Neurophysiology.* 23:315–338.